Journal of Sound and Vibration 370 (2016) 176–190

Contents lists available at ScienceDirect

Journal of Sound and Vibration

journal homepage: www.elsevier.com/locate/jsvi

Characterisation of wind farm infrasound and low-frequency noise

Branko Zajamšek [a,*], Kristy L. Hansen [b], Con J. Doolan [a], Colin H. Hansen [c]

[a] University of New South Wales, Sydney 2052, Australia
[b] Flinders University, Adelaide 5042, Australia
[c] University of Adelaide, Adelaide 5005, Australia

ARTICLE INFO

Article history:
Received 9 September 2015
Received in revised form
19 January 2016
Accepted 1 February 2016
Handling Editor: D. Juve
Available online 15 February 2016

ABSTRACT

This paper seeks to characterise infrasound and low-frequency noise (ILFN) from a wind farm, which contains distinct tonal components with distinguishable blade-pass frequency and higher harmonics. Acoustic measurements were conducted at dwellings in the vicinity of the wind farm and meteorological measurements were taken at the wind farm location and dwellings. Wind farm ILFN was measured frequently under stable and very stable atmospheric conditions and was also found to be dependent on the time of year. For noise character assessment, wind farm ILFN was compared with several hearing thresholds and also with the spectra obtained when the wind farm was not operating. Wind farm ILFN was found to exceed the audibility threshold at distances up to 4 km from the wind farm and to undergo large variations in magnitude with time.

1. Introduction

Annoyance due to wind farm low-frequency noise (commonly defined between 20 and 200 Hz, although sometimes defined between 20 and 160 Hz) is often reported [1–4] yet there are no comprehensive data concerning wind farm low-frequency noise characteristics or how meteorological conditions affect these characteristics. Whether or not wind farm infrasound contributes to annoyance is widely debated and there is no current consensus.

It has been suggested by Van den Berg [5] that blade–tower interaction could be responsible for wind farm infrasound. According to Van den Berg [5], the wind passing over the tower creates a region of velocity deficit in front of the tower, which causes temporal changes in angle of attack, resulting in *thickness noise* at the blade pass frequency. More recently, the idea of BTI noise has been further evaluated by Doolan et al. [6] who propose a first-order aerodynamic model to simulate the BTI and then use the theory by Curle [7] to estimate the far field acoustic pressure. The changes in angle of attack result in unsteady lift at the blade-pass frequency (BPF) which causes tonal ILFN (commonly called BTI noise) with the characteristic tones at the BPF and upper harmonics. This is somehow analogous to BTI noise from downwind turbines [8] but it is not as well studied or recognised for modern upwind wind turbines. Other possible sources of unsteady lift and thus wind farm ILFN are cross-winds, atmospheric turbulence and wind shear. These aerodynamic sources could generate *loading noise*, which also manifests itself at the BPF and upper harmonics [9]. Although possible, the mechanisms of BTI noise and

* Corresponding author.
E-mail addresses: b.zajamsek@student.unsw.edu.au (B. Zajamšek), kristy.hansen@flinders.edu.au (K.L. Hansen), c.doolan@unsw.edu.au (C.J. Doolan), colin.hansen@adelaide.edu.au (C.H. Hansen).

http://dx.doi.org/10.1016/j.jsv.2016.02.001
0022-460X/

loading noise have not yet been experimentally verified on a wind turbine and therefore the degree to which they influence wind farm ILFN production remains unknown. Another possible source of wind farm ILFN is stall noise, which is assumed to occur under stable atmospheric conditions [10]. Stall noise is likely the source of "other" amplitude modulation [11], although it is not clear that it generates infrasound or low-frequency noise tonal components at the blade-pass frequency.

Since wind farms operate in the atmospheric boundary layer, an influence of boundary layer characteristics, such as wind shear and stability, on wind farm ILFN is expected. Van den Berg [12], who correlated wind farm noise with meteorological stability measured 40 km away from a wind farm, hypothesised that a stable atmosphere has a significant effect on wind farm noise emissions that occur during the night. This conclusion is based on stable atmospheric velocity profile characteristics; a low wind speed at ground level, which causes low ambient noise levels, and a relatively high wind speed at the hub height, which causes high levels of wind farm noise generation. The importance of atmospheric stability has also been shown by Hansen et al. [13] who correlated low-frequency wind farm noise at dwellings with atmospheric stability calculated from wind speeds at a height of 1.5 m (measured at dwellings) and at hub height. Hansen et al. [13] concluded that wind farm noise is most noticeable under stable atmospheric conditions and in the downwind direction.

Studies regarding wind farm infrasound emissions conducted by Jakobsen [14], Van den Berg [5], Turnbull et al. [15] and O'Neal et al. [16] all conclude that the levels of wind farm infrasound emissions are too low to be audible at typical closest distances to residences, although it is possible that the infrasound part of the spectrum may be audible close to a wind turbine. On the other hand, measurement of low-frequency noise by Hansen et al. [13] and Jung et al. [17] show that wind farm low-frequency noise exceeds the normal hearing threshold. Further, Møller and Pedersen [18] in their comprehensive review also show that wind farm low-frequency noise (63–250 Hz in their study) is audible and they postulated an increase in wind farm low-frequency noise with the future increase in wind turbine size. In a recent paper by Marcillo et al. [19], wind farm infrasound was measured up to 50 km away from the wind farm. The capacity for wind farm infrasound being able to travel that far is attributed in that paper to several factors such as stable atmospheric conditions and atmospheric sound waveguides produced as a result of wind shear in a stable atmosphere. No literature has been found that addresses the correlation between atmospheric stability measured at the wind farm location and wind farm ILFN characteristics. This paper thus presents an original experimental investigation that links detailed atmospheric conditions at a wind farm location with wind farm ILFN characteristics and occurrence at dwellings. Specifically, two questions are addressed: (a) what are the unique acoustic characteristics of wind farm ILFN at dwellings and (b) how often and under which atmospheric conditions is wind farm ILFN present at dwellings?

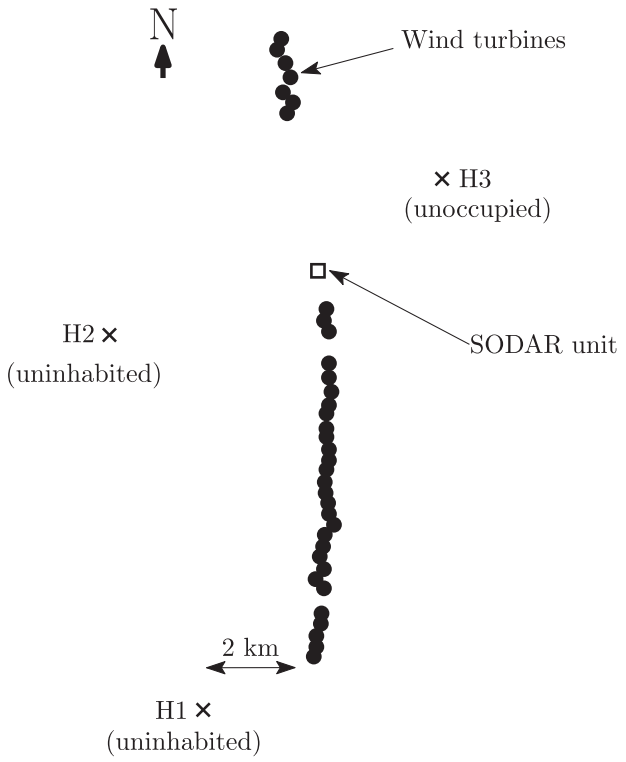

Fig. 1. Measurement and SODAR locations with respect to the wind farm.

2. Methodology

2.1. Measurement locations

Measurements were carried out at two uninhabited and one unoccupied (for the duration of the measurements) dwellings in the close vicinity of the Waterloo wind farm for 15 days in total during the Australian autumn and winter. The wind farm is located in South Australia, which has a "Mediterranean" type of weather with mild wet winters (average maximum temperature of 14 °C and average rainfall of 80 mm) and hot dry summers (average maximum temperature of 29 °C and average rainfall of 26 mm). The uninhabited dwellings had all doors and windows intact, and are sparsely furnished. The dwellings will be referred to as measurement locations H1, H2 and H3, respectively, indicated in Fig. 1, together with the wind turbines and SODAR unit. In general, there was no significant extraneous sound sources nearby the measurement locations, except countryside roads, farming activity and a small size quarry at location H2, which was located approximately 400 m away from the measurement set-up.

For location H1, the measurement period was from 8/05/2013 to 13/05/2013 (autumn); for location H2 from 1/05/2013 to 3/05/2013 (autumn); and for location H3 from 24/7/2013 to 1/08/2013 (winter). Locations H1 and H3 are approximately 3 km away from the nearest wind turbine and location H2 is approximately 4 km away from the nearest wind turbine. The wind farm is made up of 37 wind turbines each of rated power 3 MW, 90 m hub height and 90 m rotor plane diameter. The wind farm is located on a ridge and therefore the average height of the wind turbine base is 200 m above measurement locations H1–H3. The rural environment surrounding the wind farm is relatively flat with sparse low hills and farm fields. Measurements were undertaken when the wind farm was operating and non-operating. The wind farm operational state was determined from the wind farm power output capacity factor which is calculated as the ratio between the maximum and actual wind farm power output expressed as a percentage. At all locations the acoustic measurements were taken indoors and outdoors. A schematic of the measurement set-up at all three locations is shown in Fig. 2.

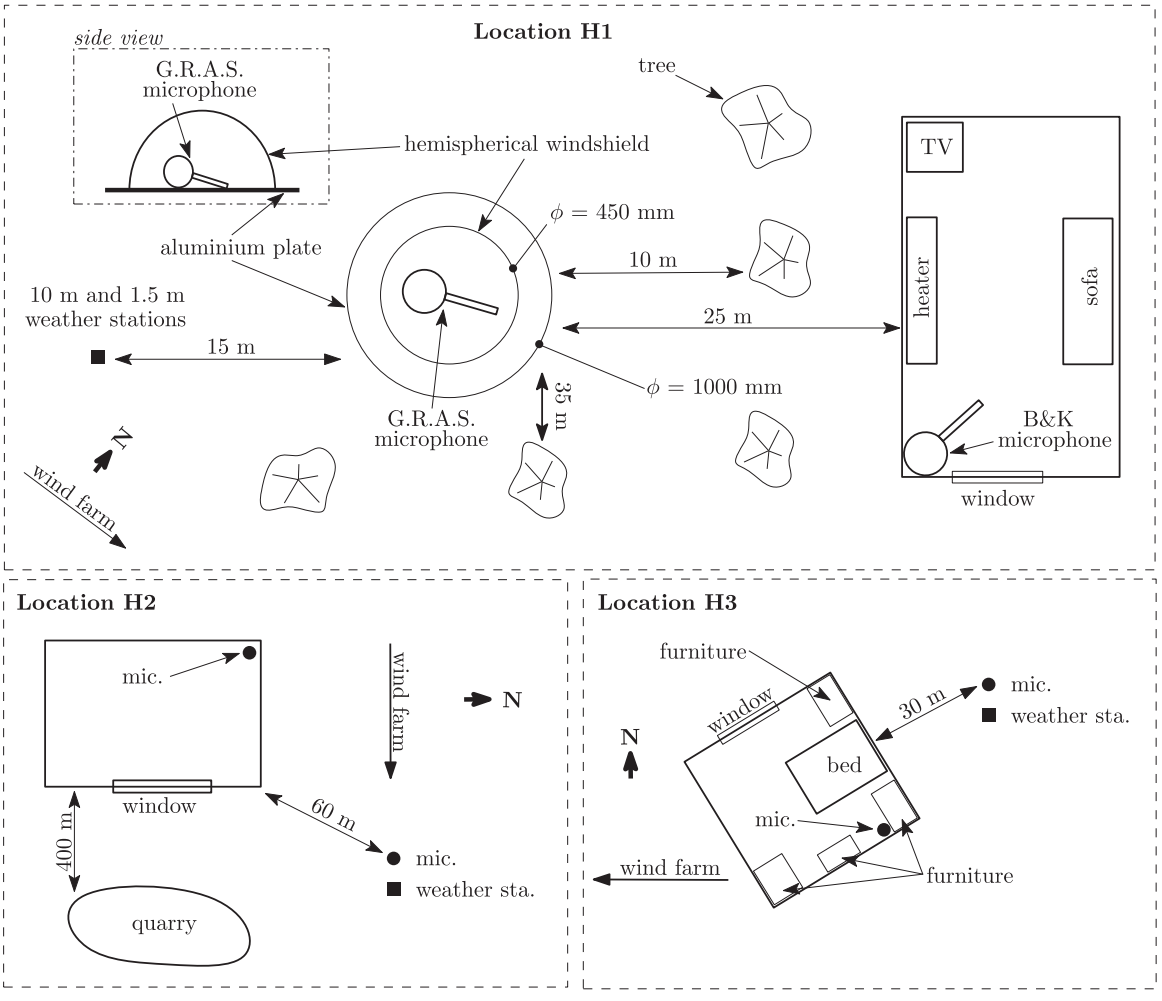

Fig. 2. Schematic diagram of the measurement set-up at locations H1–H3. Letter ϕ stands for diameter.

At location H1, the outdoor microphone was placed approximately 25 m away from the dwelling and was surrounded by some trees (5 m high) located at least 10 m away as shown in Fig. 2. Weather stations at heights 1.5 and 10 m were placed 40 m away from the house and approximately 35 m from the nearest trees. The indoor microphone was located in a corner of a room that contained a sofa, fire place and television. At location H2, the indoor microphone was placed inside an unoccupied house in the corner of an empty room which had a window facing the wind farm. Weather stations at heights 1.5 m and 10 m were located in an open field approximately 60 m away from the dwellings, the outdoor microphone was positioned nearby. At location H3, the indoor microphone was positioned in a bedroom. The outdoor microphone and weather stations at this location were placed 30 m away from the dwelling. The outdoor microphone at all three locations was placed in a primary 90 mm spherical windshield and then in a secondary hemispherical windshield. The hemispherical windshield consists of 3 mm thick and 1 m diameter aluminium plate and the microphone is placed in the centre of this plate. The secondary windshield is attached to the plate and consist of a 16 mm layer of acoustic foam covered by a layer of SoundMaster acoustic fur. The foam and fur are supported by a 450 mm diameter steel frame of hemispherical shape made out of thin-wire steel. The hemispherical design follows the specifications in the IEC 61400-11:2012 standard [20]. An acoustic evaluation of this windshield can be found in Hansen et al. [13]. The weather stations were not surrounded by any vegetation or any other kind of high obstructions.

2.2. Instrumentation

Time series data from the indoor microphones were recorded using a B&K LAN-XI 24 bit data acquisition card, which was operated using Pulse software. The data on this device were recorded at a sampling rate of 8192 Hz. The outdoor microphones on the other hand were connected to a National Instrument 9234, 24-bit data acquisition card with a sampling frequency of 10,240 Hz. The sampling frequencies were chosen to be relatively low, since wind farm noise is biased towards the lower frequencies and its contribution at frequencies above 2 kHz is negligible at the large propagation distances considered here.

For measuring low and infra-sonic frequency noise, a G.R.A.S. type 40AZ 1/2 in microphone with a 20 CG G.R.A.S. pre-amplifier and a B&K type 4955 1/2 in microphone were used. The G.R.A.S. microphone has a flat frequency response from 0.5 Hz to 20 kHz, noise floor of 17 dBA and it was used for the outdoor measurements. Temperature and humidity variations over the 24 h daytime/night-time cycle are assumed to have no effect on the performance of this microphone [21]. The B&K has a 6.5 dBA noise floor, flat frequency response from 6 Hz to 20 kHz and it was used for the indoor measurements. The microphone frequency response at the lower end was corrected in the frequency domain based on a previous data set. In that data set, both the B&K microphone and the G.R.A.S. microphone were positioned within the same room. Due to the large wavelengths at infrasonic frequencies, the measured infrasonic noise is the same, regardless of microphone position, within a room. Therefore, one-third-octave bands and narrowband power spectral density (PSD) levels were averaged over 20 measurements for both microphones and the B&K measurements were subtracted from the G.R.A.S. measurements to determine the correction values. All windows and doors were closed during these measurements to minimise the effect of wind-induced noise.

The wind speed and direction at heights of 1.5 m and 10 m were measured using Davis Vantage Vue and Davis Vantage Pro weather stations, respectively, and averaged over 10 min time intervals. The wind speed and direction accuracy of the weather stations is of the order of ± 0.4 m/s and 22.5°, respectively.

For profiling the atmospheric boundary layer at the wind farm location, a Fulcrum 3D SODAR (Sonic Detection and Ranging) unit was employed. The SODAR system was located between the north and south clusters of the wind turbines as shown in Fig. 1. The SODAR system was located in a clearing of stunted eucalyptus with heights up to 10 m. The trees are approximately equidistant from the SODAR at a distance of around 10 m. Positioning was such that the environment had minimal effect on the measurements (no transducer ringing). The SODAR provided wind speed and wind velocity in 10 min averages at heights ranging from 50 m to 150 m in steps of 10 m, which spans most of the rotor plane. The wind speed and direction resolution according to the manufacturer are 0.01 m/s and 0.1°, respectively. The manufacturer also reports an accuracy in terms of correlation coefficient between the SODAR and a weather mast, which is 0.98. Since the unit was positioned on top of the ridge, it should be taken into account that the velocity profile on the ridge might be affected by the corresponding variation in ground height.

The hub height wind speed and direction data were provided by the wind farm operator for the time period from 1/4/2013 to 24/6/2013 in 10 min averages. Waterloo wind farm output power information was obtained from the Australian Energy Market Operator website [22] in 5 min averages.

2.3. Analysis techniques

In previous investigations of wind farm ILFN by Hansen et al. [13] it was found that the Waterloo wind farm acoustic signature consists of a 0.8 Hz BPF (limited by 0.1 Hz frequency resolution) and higher harmonics. In order to capture the occurrences of wind farm ILFN, a peak detection algorithm was designed that searches for a peak at the fourth blade-pass frequency harmonic (3.2 Hz) in the PSD spectra which was calculated over a 10 min time block (as described in the next paragraph) and had 0.1 Hz frequency resolution. The algorithm was applied on the indoor time data obtained by the B&K microphone. If the 3.2 Hz peak was at least 20 dB above the broadband noise level then the 3.2 Hz peak magnitude was

captured. The broadband nose level was defined as the base of the trough between the 3.2 and 4 Hz peak. The 20 dB dynamic range was chosen arbitrarily in order to capture the instances when the infrasound presence was significant. With this method of detecting the infrasound, a compromise has been made between ensuring that the infrasound can be attributed to the wind farm and that all peaks (including those masked by wind-induced noise) are detected. Additionally, it was found that the occurrence of variation in BPF and 4th harmonic frequency is insignificant and thus no correction for the frequency variation at the 4th harmonic was necessary.

The narrow-band power spectral density (PSD) estimation was calculated using Welch's averaged modified periodogram method of spectral estimation with a Hanning window of length 81,920 ($10\times$ the sampling frequency) points and 50 percent overlap which gives a 0.1 Hz frequency resolution. The PSD was also corrected for windowing and frequency resolution effects in the following way according to Randall [23]:

$$\mathrm{PSD}_{\mathrm{corrected}} = \mathrm{PSD} + \log_{10}(B_{\mathrm{en}} \times \Delta f), \tag{1}$$

where B_{en} is the normalised noise bandwidth (1.5 for the Hanning window) and Δf is the frequency resolution.

When possible (at location H1 and H2) the indoor microphone was positioned in a corner of the room. This is because in the corner all room modes will have anti-nodes (regions of high acoustic pressure) which might also occur at another location in the room. The spatial position of anti-nodes at positions other than the room corner will vary with the frequency of the mode. The corner measurements therefore represent worst case conditions [24]. All acoustic results were obtained from 10 min long time blocks (unless otherwise specified).

The atmospheric stability was determined from the shear exponent factor, m, which is defined as

$$m = \frac{\ln(v_h/v_{\mathrm{ref}})}{\ln(h/h_{\mathrm{ref}})}, \tag{2}$$

where v_h is the wind speed at height h (126 m, top of the rotor plane) and v_{ref} is the wind speed at a reference height h_{ref} (36 m, bottom of the rotor plane). The wind speed data for calculating the m-factor were obtained from SODAR measurements at 40 and 130 m heights. The relationship between atmospheric stability and the shear exponent factor is tentative and herein the relationship as defined by Van den Berg [25] is used and is shown in Table 1. This table also provides the Monin–Obukhov length [25], which is a classical stability parameter, for the purposes of comparison.

The year was divided into meteorological seasons, with summer, autumn, winter and spring beginning on the first day of December, March, June and September, respectively. Night-time is specified as the time between 11 pm and 7 am. This definition is chosen due to farming activity which occurs in the region during the daytime since this is a source of extraneous noise. Night time is defined between 11 pm and 7 am in several jurisdictions – in the UK, the Netherlands and Italy [26].

3. Results

3.1. Noise character

Fig. 3 shows a comparison between ON/OFF measurements of indoor and outdoor PSD at locations H2 and H3. The OFF case conditions were matched to the ON case conditions via wind speed at 1.5 m as shown in Table 2 and time of the day as shown in Figs. 11 and 12. Comparison between the ON/OFF cases in Table 2 reveals that the measurement location H3 was positioned downwind from the wind farm and that the measurement location H2 was positioned in a cross-wind direction relative to the wind farm. These parameters show that the meteorological conditions at the time when the wind farm was ON/OFF were similar and thus the differences in PSD between the ON/OFF cases in Fig. 3 can be attributed to wind farm noise only.

As shown in Fig. 3, the main difference between the ON/OFF indoor and outdoor cases is the presence of the BPF tones at 0.8 Hz and higher harmonics up to 6 Hz, and humps at around 30 Hz and 50 Hz. The presence of 0.8 Hz is not clearly seen in Fig. 3 (as well as in Fig. 4), which is attributed to the actual wind farm noise characteristic and not the B&K microphone frequency response because (a) 0.8 Hz is not measured by the G.R.A.S. microphone either which has a flat frequency response above 0.5 Hz (not shown), (b) the fundamental BPF is not expected to be of the highest magnitude when the source of noise is unsteady according to Hubbard [27] and thus it could be masked by the background noise in Fig. 3b, (c) the fundamental BPF has been previously measured with the G.R.A.S. microphone where the BPF was found to be at lower level

Table 1
Atmospheric stability, shear exponent factor, m, and Monin–Obukhov length.

Atmospheric stability	Shear exponent m range	Monin–Obukhov length, L
Unstable	$m \leq 0.1$	
Neutral	$0.1 < m \leq 0.2$	$700\ \mathrm{m} < L$
Stable	$0.2 < m \leq 0.4$	$100\ \mathrm{m} < L < 700\ \mathrm{m}$
Very stable	$m > 0.4$	$0\ \mathrm{m} < L < 100\ \mathrm{m}$

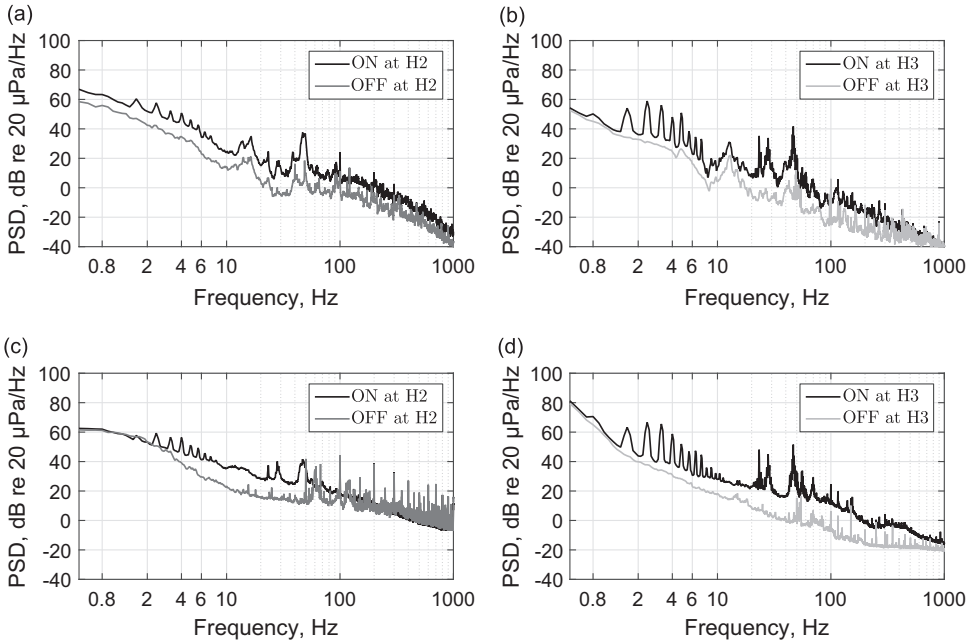

Fig. 3. Comparison between the indoor and outdoor ON/OFF power spectral density (PSD). The time when these measurements were taken is marked in Figs. 11 and 12. (a) Location H2 indoor, (b) location H3 indoor, (c) location H2 outdoor and (d) location H3 outdoor.

Table 2
Conditions associated with the wind farm being ON/OFF for locations H2 and H3.

ON/OFF condition and location	Wind speed @ 1.5 m and hub height (m/s)	Wind direction @ 1.5 m and hub height	Capacity factor (%)
ON at H2	1.5 ± 0.4, 15	NE, NE	76
OFF at H2	1.5 ± 0.4, 9.9	SE, SE	0
ON at H3	0 ± 0.4, 10.3	W, W	50
OFF at H3	0 ± 0.4, 1.4	NW, NW	0

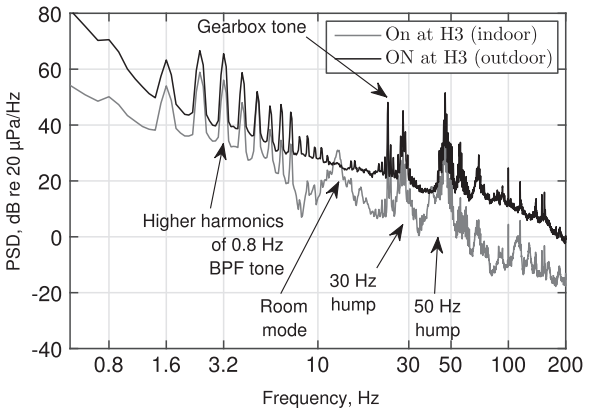

Fig. 4. Comparison between the indoor/outdoor power spectral density at location H3. The time when these measurements were taken is marked in Fig. 12 ("ON at H3" vertical line).

in comparison to the second and third BPF higher harmonic [13] and (d) the B&K microphone frequency response was corrected for a roll off at the lower frequency end as described in Section 2.2. This is a typical wind turbine noise signature for this wind farm and is observed for all instances when strong infrasound was detected in Figs. 10–12. A similar PSD is also observed at location H1 (not shown). Sharp peaks at 50 Hz and higher harmonics in Fig. 3c OFF case data are attributed to electrical noise.

Additionally, a broadband hump between 10 Hz and 20 Hz is also present in Fig. 3a and b and its origin is attributed to an acoustic mode associated with the room dimensions [28]. Comparison between the indoor and outdoor results for the ON

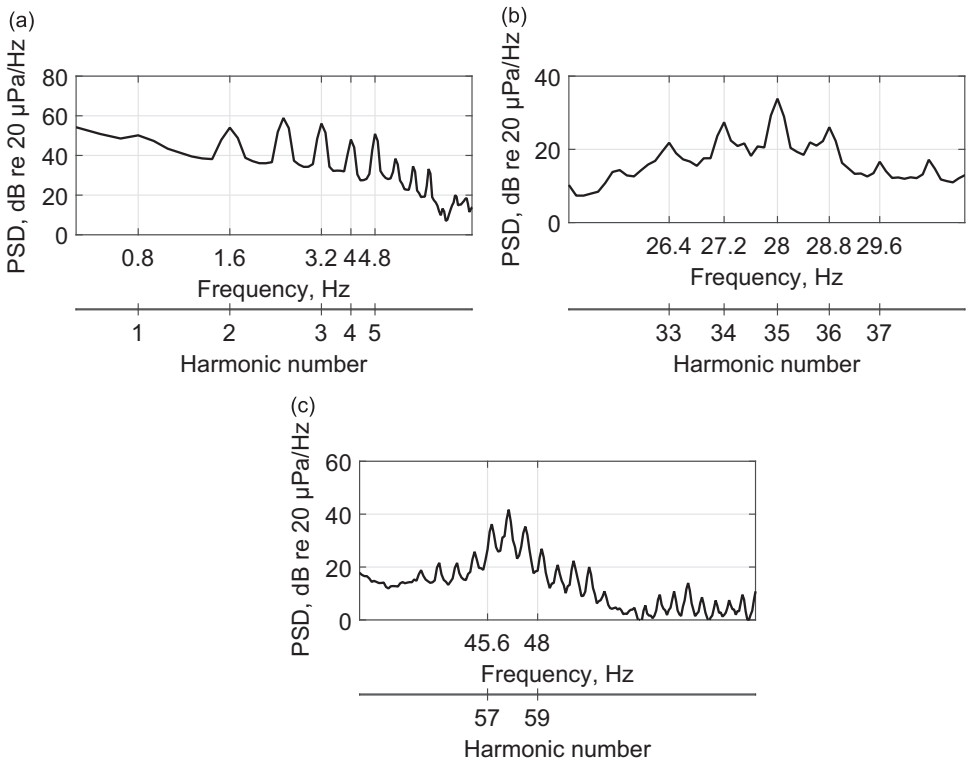

Fig. 5. Indoor power spectral density (PSD) at location H3 focused on three frequency ranges. The harmonic number plotted on the *x*-axis is based on 0.8 Hz BPF. The time when these measurements were taken is marked in Fig. 12 ("ON at H3" vertical line).

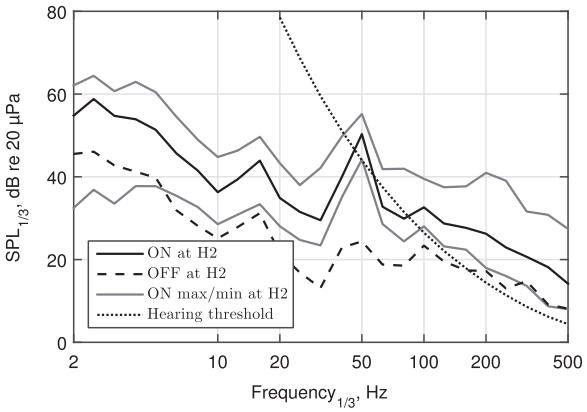

Fig. 6. Comparison between the worst case (corner microphone) ON/OFF conditions at location H2 (indoors), and the normal hearing threshold as specified in ISO 226-2003 [30]. The time when these measurements were taken is marked in Fig. 11.

case at location H3 (see Table 2 for details), as shown in Fig. 4, confirms this, since the hump between 10 Hz and 20 Hz only occurs indoors. Lower indoor levels over the whole frequency range are attributed to noise attenuation caused by the house and are as expected [28]. The higher outdoor levels below 2 Hz are likely due to wind induced noise on the outdoor microphones as the house noise reduction is zero at these frequencies [28]. Note that wind induced noise is also very likely to be present at location H3, since a wind speed of 0 m/s is not certain due to the ± 0.4 m/s weather station precision.

In Fig. 4 an additional and commonly observed spectral characteristic is present; a sharp peak at 23 Hz in both the indoor and outdoor results. This peak is attributed to gearbox noise which is expected to occur at this frequency according to Sawalhi and Randall [29].

A closer look at the humps at 30 Hz and 50 Hz is shown in Fig. 5, where the indoor PSD from Fig. 4 is plotted against frequency and harmonic number based on a blade-pass frequency estimation of 0.8 Hz. From Fig. 5 it is evident that the peaks in the infra-sonic region as well as around 30 Hz and 50 Hz are higher harmonics of the blade-pass frequency, 0.8 Hz. A noticeable misalignment is noted at higher harmonic numbers in Fig. 5c, which are due to currently unknown reasons. A

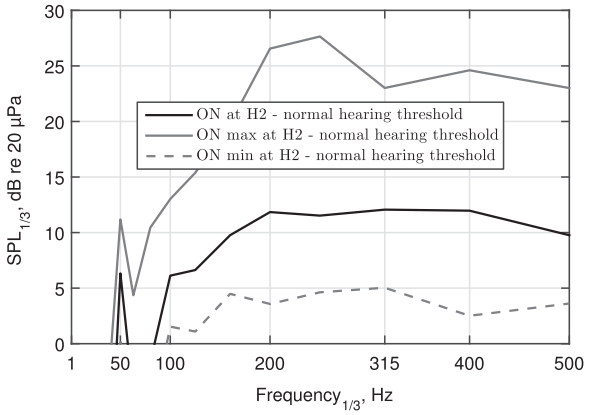

Fig. 7. Indoor ON case conditions normalised by the normal hearing threshold at location H2. The time when these measurements were taken is marked in Fig. 11 ("ON at H2" vertical line).

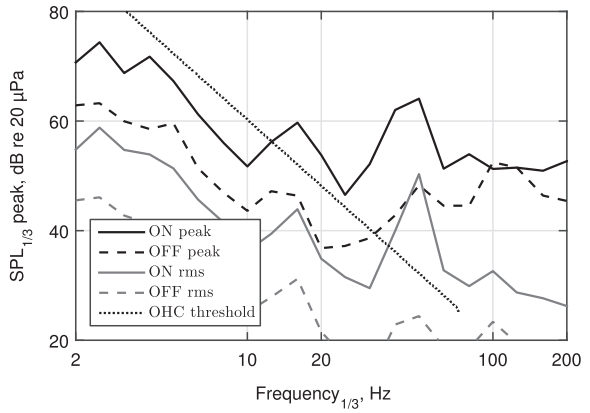

Fig. 8. Comparison of indoor rms and peak one-third-octave band sound pressure level at location H2 with the OHC threshold from Salt and Hullar [34]. The time when these measurements were taken is marked in Fig. 11.

possible explanation for the misalignment could be an accumulation of errors resulting from small variations in the blade-pass frequency. However, information about the rotational speed of wind turbines was not available and hence this could not be verified.

Fig. 6 shows the worst case ON/OFF conditions at location H2 (indoors) compared with the normal hearing threshold according to ISO 226-2003 [30]. The ISO 226 hearing threshold represents the median value of the normal hearing threshold of young adults (18–25 years) for pure tones and binaural listening. The noise contribution in the infrasonic range is below the hearing threshold, which is as expected [14]. As can be seen, the wind farm low-frequency noise exceeds the normal hearing threshold curve at 50 Hz and remains above the normal hearing threshold curve throughout the whole low-frequency region up to 200 Hz.

In determining the audibility and possible annoyance capacity of wind farm noise above the 50 Hz one-third-octave band centre frequency, a number of issues must be considered. The standard deviation of the hearing threshold is considered to be between 5 and 6 dB which means that the noise in one-third-octave bands above 50 Hz, which is more than 6 dB above the threshold, will effect everybody in the population between 18 and 25 years old. Additionally, the importance of the 50 Hz one-third-octave band centre frequency on the overall loudness sensation is unclear, since each one-third-octave band above the 50 Hz band exceeds the hearing threshold by a comparable or greater amount that it does at 50 Hz, as can be seen in Fig. 7. In this figure the indoor ON case at H2 and its max/min variations are normalised by the ISO 226 hearing threshold which shows that the peak at 50 Hz and the noise level in higher one-third-octave bands are above the normal hearing threshold approximately 6 dB and 7–12 dB, respectively. On the other hand, results from a recent EPA study [31] indicated that residents complained about a "rumbling" noise which is consistent with the presence of a 50 Hz amplitude modulated tone.

The spectra shown in Fig. 6 can be annoying (or perhaps more easily perceived) due to the time varying amplitude [32], which is indicated by the large variation of ON min/max sound pressure level for the ON conditions. The time variation of the ON case was calculated over 10 min of data in 1 s intervals. The variation in level at each one-third octave band is represented by the ON max/min curve. To conclude, the question of which one-third-octave-band centre frequency would

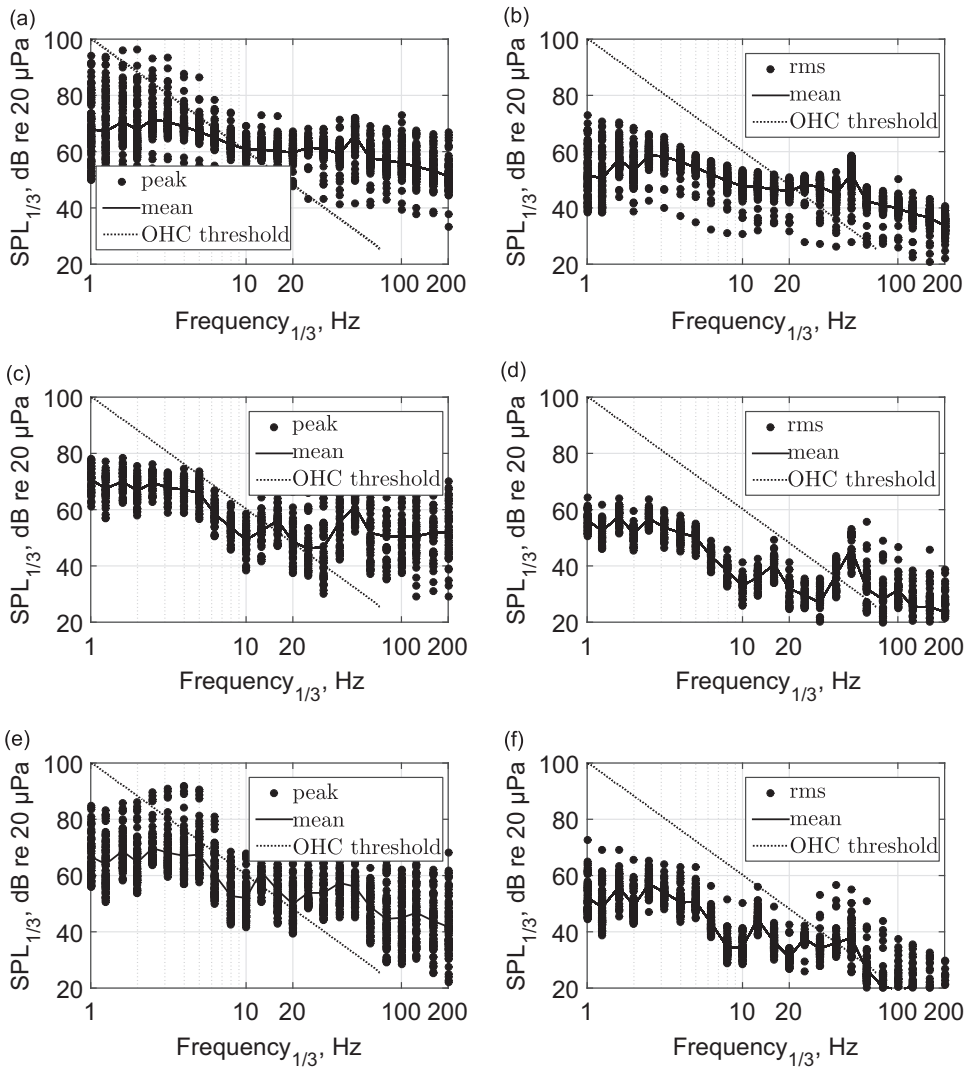

Fig. 9. Comparison of indoor peak and rms one-third-octave band centre frequency sound pressure level variations at 4th BPF occurrences at all three locations compared against the OHC threshold from Salt and Hullar [34]. (a) and (b) location H1 (peak and rms, respectively), (c) and (d) location H2 (peak and rms, respectively), (e) and (f) location H3 (peak and rms, respectively).

contribute the most to the annoyance in terms of amplitude modulation and loudness sensation remains open. Apart from annoyance, sleep disturbance could also occur due to consistent exceedance of the hearing threshold as well as the presence of tonality and magnitude variations as suggested by Hume et al. [33].

Fig. 8 shows indoor peak and rms one-third-octave band centre frequency SPL for the ON/OFF case and its comparison to the outer hair cell (OHC) threshold as specified in Salt and Hullar [34]. Salt and Hullar [34] proposed a threshold for infrasonic frequencies at which the OHCs are excited and thus cause a physiological disturbance in the ear. In Fig. 8 it can be seen that wind farm infrasound is significantly higher in comparison to the OFF cases which suggests that the wind farm is a noticeable source of infrasound. Further, wind farm infrasound does not exceed the OHC threshold in the 1–12.5 Hz one-third octave band range. However, the peak sound pressure level exceeds the OHC threshold between the 12.5 Hz and 20 Hz one-third octave band but the noise in that range is somewhat amplified as it excites room modes (see Fig. 4). The rms sound pressure level does not exceed the OHC threshold in the infrasonic range. These results therefore suggest that the peak wind farm infrasound at dwellings 4 km away from the wind farm can have a physiological effect on the ear at frequencies corresponding to acoustic room resonances.

Fig. 9 shows a comparison between indoor peak and rms one-third-octave band centre frequency sound pressure level and the OHC threshold for when the wind farm was on at all three locations. The mean value of the peak and rms levels is indicated by the solid black lines in the figures. The rms sound pressure levels shown in Fig. 9b, d, f in general do not exceed the OHC threshold below 20 Hz. On the other hand, the peak sound pressure levels exceed the OHC threshold at all three

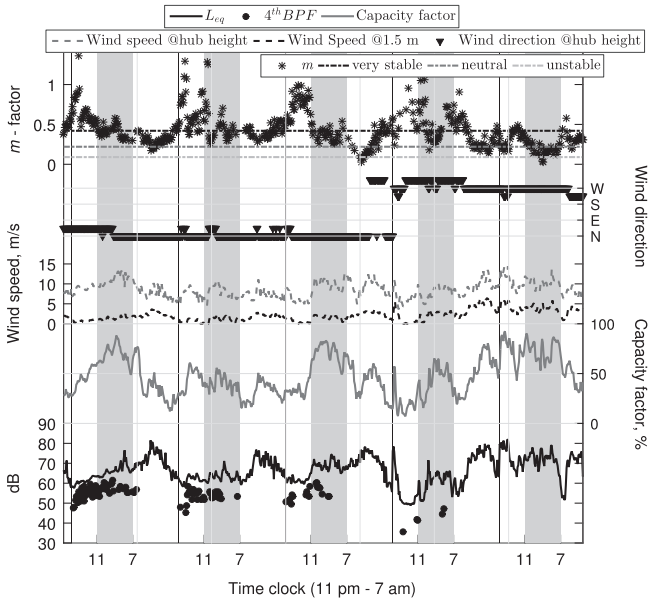

Fig. 10. Comparison between the 4th BPF harmonic sound pressure level (indoor), L_{eq} (indoor), wind farm capacity factor, wind speed at 1.5 m and hub height, wind direction at hub height and wind shear exponent factor, m, for location H1. Vertical black lines indicate sunset time at 5.15 pm and the grey area indicates night time between 11 pm and 7 am. The measurement period spanned from 8/05/2013 to 13/05/2013. The hub height wind speed and direction were obtained from the wind farm operator.

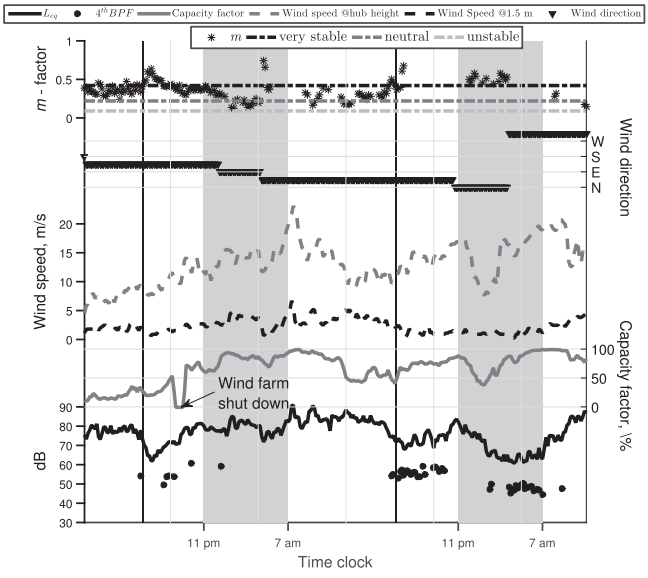

Fig. 11. Comparison between the 4th BPF harmonic sound pressure level (indoor), L_{eq} (indoor), wind farm capacity factor, wind speed at 1.5 m and hub height, wind direction at hub height and wind shear exponent factor m at location H2. Vertical black lines indicate sunset time at 5.15 pm and the grey area indicates night time between 11 pm and 7 am. The measurement period spanned from 1/05/2013 to 3/05/2013. The hub height wind speed and direction were obtained from the wind farm operator.

locations; the lowest exceeded frequency is 1.6 Hz in Fig. 9a. The mean peak sound pressure levels exceed the OHC threshold between 10 and 20 Hz at all three locations.

3.2. Acoustical and meteorological conditions

Fig. 10 shows the occurrences of wind farm infrasound marked as 4th BPF, together with the L_{eq}, wind farm capacity factor, wind speed/direction and shear exponent factor m. From the wind farm capacity factor plot, it is evident that the wind farm was operating for the whole duration of the measurements. The wind direction plot shows that the H1

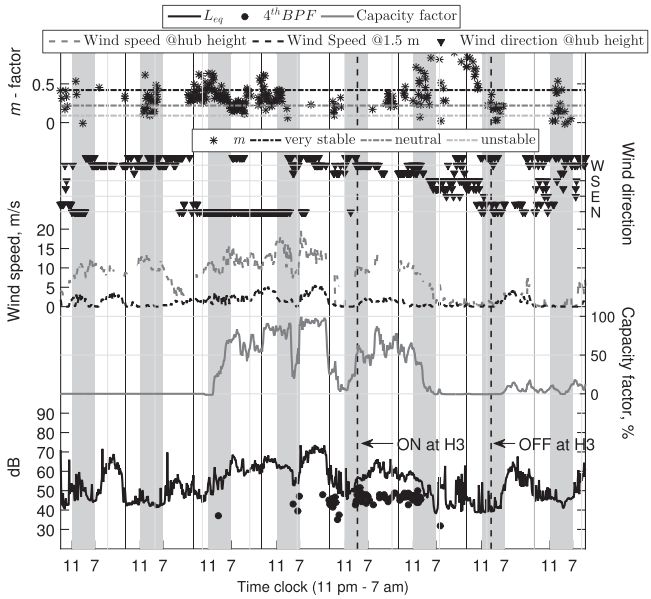

Fig. 12. Comparison between the 4th BPF harmonic sound pressure level (indoor), L_{eq} (indoor), wind farm capacity factor, wind speed at 1.5 m and hub height, wind direction and stability factor, m, at location H3. Vertical black lines indicate sunset time at 5.15 pm and the grey area indicates night time between 11 pm and 7 am. The measurement period spanned from 24/7/2013 to 1/08/2013. The hub height wind speed and direction were obtained from SODAR.

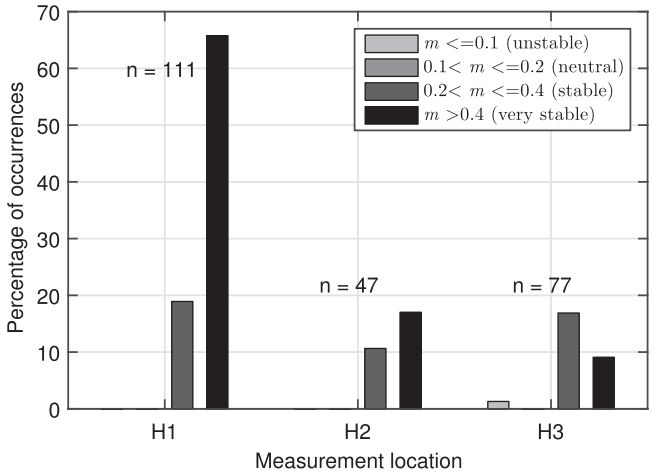

Fig. 13. Variation of 4th BPF occurrence with atmospheric stability. The parameter n indicates the total number of 4th BPF occurrences at each measurement location.

measurement location was downwind from the wind turbines within 5 km and South-West from the wind turbines between 5 km and 9 km distant, during the first three nights.

Fig. 10 shows that the wind farm consistently produces infrasound immediately after sunset and during the night for the first three days. From visual inspection of the spectra for all instances of the 4th BPF, it was found that infrasound is always accompanied by low frequency noise containing distinct tonal components concentrated around 30 and 50 Hz. The typical ILFN at the 4th BPF is thus similar to the one shown in Figs. 4 and 5. Atmospheric stability can be deduced from the wind shear exponent factor m (see Table 1 for the relation between the wind shear factor and atmospheric stability). Variations in the m-factor show that the atmosphere transitions from neutral to stable just after sunset and remains stable until 7 am. At some instances, unexpectedly high (>0.6) m-factor values are observed in Fig. 10 (the same is also true for Figs. 11 and 12) and could be caused by low level jets [35] or the effect of the ridge on the velocity profile. Fig. 10 thus suggests a relationship between a very stable atmosphere ($m > \sim 0.42$) at the wind farm location, down-wind conditions and wind farm tonal ILFN at a dwelling (H1), which is located $\sim$4 km away from the nearest wind turbine.

Fig. 11 shows the instances of 4th BPF harmonic SPL together with the L_{eq}, wind farm capacity factor and meteorological variables at measurement location H2. During the measurements at location H2, a one hour long wind farm shut down

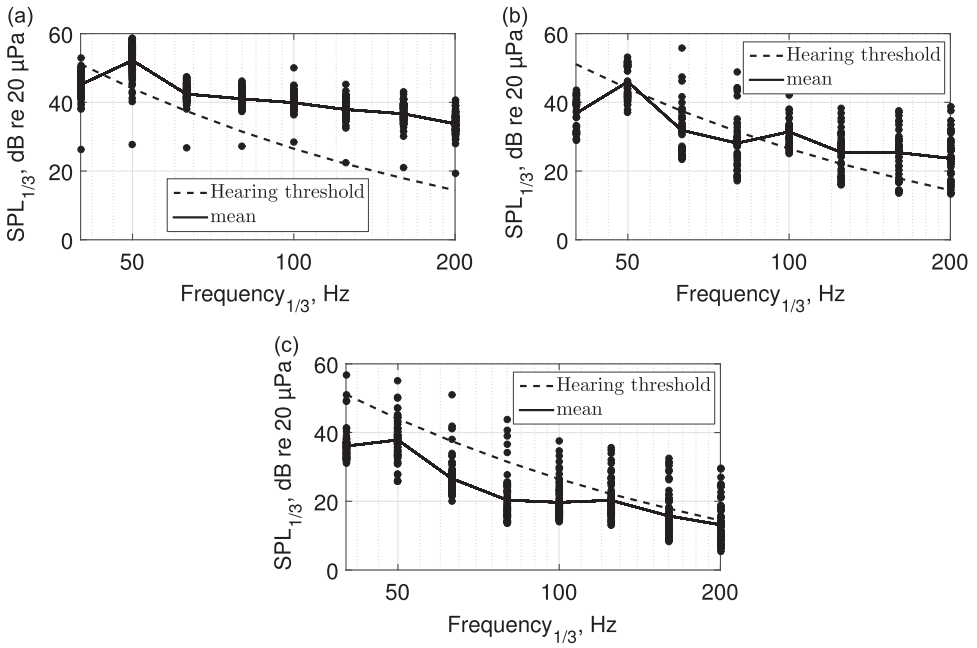

Fig. 14. Indoor one-third-octave band centre frequency ILFN variation at 4th BPF occurrences. (a) Location H1, (b) location H2 and (c) location H3.

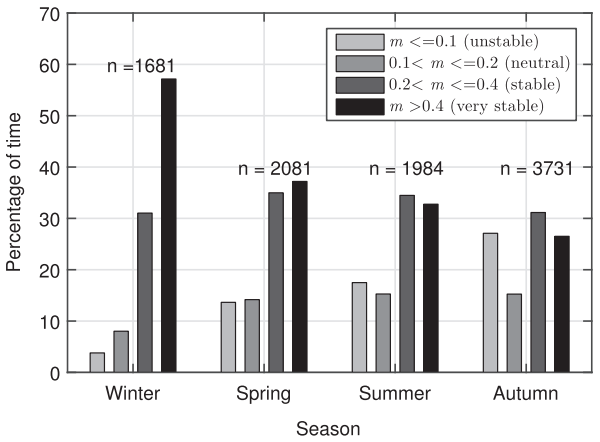

Fig. 15. Variation of atmospheric stability throughout four seasons in the year 2013. The parameter *n* indicates the total number of samples for each season.

occurred around 8.20 pm on the first of May 2013. The shut down time is clearly marked by a sudden drop in wind farm capacity factor shown in Fig. 11. According to the limited amount of *m*-factor data (in general available only for the first day and night) it can be concluded that the occurrence of ILFN follows a similar trend as the one already seen in Fig. 10. This conclusion must be taken with caution due to low amount of *m*-factor data. However, as can be seen in Fig. 11, the 4th BPF is also present during the second day after sunset when the wind blows from the North (N) and West (W) which puts the location H2 in an upwind/crosswind position. This seems to suggest that the ILFN is not strongly dependent on wind direction, since the 4th BPF was detected when the measurement location was positioned in the downwind, upwind and crosswind directions relative to the wind farm.

Fig. 12 shows instances of wind farm infrasound (4th BPF harmonic), L_{eq}, wind farm capacity factor and meteorological variables for the measurement location H3. As can be seen by the 0 percent capacity factor values in Fig. 12, extended periods of wind farm shut down occurred. For the period when the wind farm was operating, the 4th BPF was measured both during the day and night when the wind was mostly blowing from the West (downwind conditions). Although it is not immediately obvious from Fig. 12, the majority of the 4th BPF occurrences (for which *m*-factor data are available) correspond to stable and very stable atmospheric conditions (see Fig. 13).

For ease of comparison, the percentage of 4th BPF occurrences is plotted in Fig. 13 for each measurement location as a function of atmospheric stability. At measurement location H1, ~95 percent of the time when the 4th BPF was detected, the

atmospheric stability was classified as stable or very stable (this is found by adding the histogram values corresponding to stable and very stable). For 5 percent of the time when the 4th BPF was present, the atmospheric stability (m-factor) is missing. For measurement locations H2 and H3, it can be seen that the 4th BPF also predominantly occurs under stable and very stable conditions; ~28 percent of the time at both locations. However, a significant amount of atmospheric stability data is missing at these two measurement locations and therefore these results need to be interpreted with caution.

Fig. 14 shows the variation in the average indoor SPL in ILFN one-third-octave bands, where the data correspond to the 4th BPF occurrences that are shown in Figs. 10–12. The data from Fig. 14a reveals that for 91 percent that the 4th BPF is detected the low-frequency noise in the 50 Hz one-third-octave band exceeds the normal hearing threshold. Further, the noise in one-third-octave bands above 100 Hz exceeds the hearing threshold at all times. This finding seems to suggest that low-frequency noise, with distinct tonal components, is likely to occur and to be on average above the normal hearing threshold when infrasound is present. However, this relationship is not so clearly observed at measurement locations H2 and H3 as shown in Fig. 14b and c. At H2 in Fig. 14b the LF noise on average still exceeds the normal hearing threshold at 50 Hz and above the 100 Hz one-third-octave band while the average levels in Fig. 14c are relatively low and do not exceed the hearing threshold. Relatively low levels in Fig. 14c are attributed to the position of the microphone, which was not exactly in a corner of a room as for location H1 and H2.

Taken together, the results in Figs. 10–13 suggest that there is a relationship between wind farm infrasound and very stable atmospheric conditions. No relationship was observed between the wind direction and the occurrence of 4th BPF. The next logical step is to examine how the atmospheric stability varies throughout the year. This will give an indication of when to expect wind farm ILFN to be dominant.

3.3. Atmospheric data

Fig. 15 shows the variation in atmospheric stability calculated between heights of 40 m and 130 m (rotor plane), determined using a SODAR system (SODAR location shown in Fig. 1), for four seasons. The variation is quantified as a percentage of time during each season that the atmosphere is very stable, stable, neutral or unstable, during the night time from 5 pm to 7 am. It is apparent from Fig. 15 that the atmosphere is most often stable and least often unstable during the winter. The same trend is observed for spring and summer. The only difference in spring and summer is that the prevalence of a very stable atmosphere is less than in winter time. Interestingly in spring, summer and autumn, the prevalence of stable and unstable atmospheric conditions during the night time is similar. These significant differences between the winter and other seasons could be partially attributed to the length of the “sun up” period, which is smaller in winter. Additionally, the distribution of atmospheric stability also depends on climate zone. No literature has been found for rural Australian environments to which these atmospheric results can be compared. The most relevant results were reported by Van den Berg [25] who carried out a study in The Netherlands. However, the results cannot be directly compared due to the significant geographical differences such as the terrain profile and the location of the wind turbines. What Fig. 15 shows is that the wind farm ILFN, which tends to occur under very stable atmospheric conditions, could occur up to ~30 percent of the night time during spring, autumn and summer and up to ~60 percent of the night time during winter.

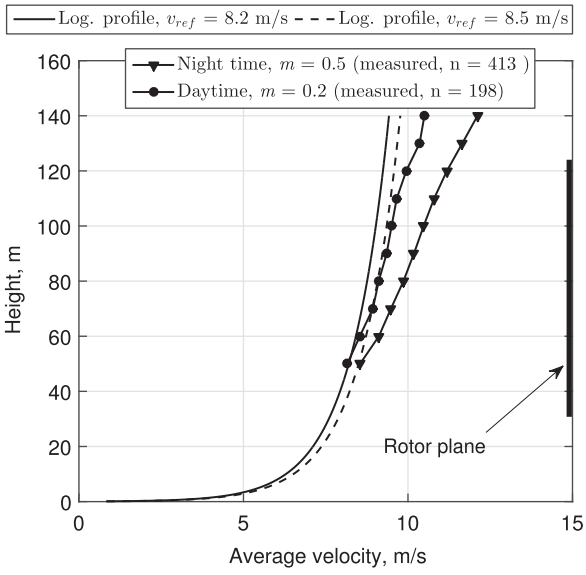

Fig. 16. Typical measured wind velocity profiles at night-time and daytime across the rotor plane, and predicted wind profile using Eq. (3) with z_0=0.05 m (assuming a rural environment with few trees [37]). The parameter n indicates the number of wind speed profiles used in calculating the average wind speed profile.

Fig. 16 shows an averaged measured wind profile (for a given m-factor) across the rotor plane using SODAR and the widely used logarithmic wind profile, which is defined as

$$v_h = v_{\mathrm{ref}} \frac{\ln(h/z_0)}{\ln(h_{\mathrm{ref}}/z_0)}, \tag{3}$$

where v_h is the velocity at height h above the terrain, v_{ref} is the reference velocity at reference height h_{ref} and z_0 is the surface roughness. The measured night-time wind profile has a steeper gradient compared to the daytime profile, which is expected according to the average m-factor values shown in Figs. 10–12. From the data in Fig. 16 it is apparent that on average, there is a higher velocity gradient in the rotor plane during the night-time. This night-time velocity profile could be the source of stall noise and have some significant effects on the BPF higher harmonics as suggested by Hubbard and Shepherd [36]. Better agreement is observed between the logarithmic wind profile and the daytime measured profile than between night-time and logarithmic wind profile.

In summary, the data show that ILFN occurs most frequently during the time when the atmosphere is very stable. However, this varies with season and it is expected that ILFN will be most prominent during the winter time when stable atmospheric conditions occur for over 60 percent of all night times. Furthermore, during winter the atmosphere can be stable during the daytime as well.

4. Conclusions

Results of an experimental investigation into wind farm infrasound and low-frequency noise (ILFN) have revealed some interesting characteristics of noise measured at dwellings in the vicinity of a wind farm.

Comparison between the acoustic spectra measured when the wind farm was operational and non-operational demonstrated that ILFN has a tonal nature and is characterised by significantly higher levels when the wind farm is operational. Analysis of wind farm ILFN showed that indoors infra-sonic rms levels are below the normal hearing threshold although peak levels can exceed the OHC threshold at some frequencies. On the other hand, indoors wind farm low-frequency noise was shown, on average, to exceed the normal hearing threshold curve in the 50 Hz one-third-octave band and above for the worst case conditions. Of course, many people will have hearing sensitivities well above and well below the 50th percentile threshold provided by ISO 226 so the results provided here are indicative only. Further, the 50 Hz one-third-octave band centre frequency showed significant variation in magnitude with time that could be perceived as annoying.

Meteorological and acoustic data demonstrated that wind farm ILFN is likely to occur under stable and very stable atmospheric conditions, which most often occur during the night-time. It has also been found that the low-frequency part of worst case (measured in a corner of a room) ILFN exceeds the normal hearing threshold for more than 90 percent of the occurrence time that infrasound was detected. Atmospheric stability was shown to be season dependent and it was observed that a very stable atmosphere can be expected for up to 60 percent of the night-time during winter.

Due to the frequent possible occurrence of ILFN at dwellings in the vicinity of a wind farm, further research is warranted to resolve the link between ILFN and its effect on health, sleep and psychological well-being.

Acknowledgements

Financial support from the Australian Research Council, Project DP120102185, is gratefully acknowledged. We are also grateful to the rural residents in South Australia who participated in this study by allowing the measurements to be carried out at their properties.

References

[1] C. Doolan, A review of wind turbine noise perception, annoyance and low frequency emission, *Wind Engineering* 37 (1) (2013) 97–104.
[2] G. Leventhall, Review: *low frequency noise. What we know, what we do not know, and what we would like to know*, *Journal of Low Frequency Noise, Vibration and Active Control* 28 (2) (2009) 79–104.
[3] E. Pedersen, K.P. Waye, Wind turbines-low level noise sources interfering with restoration? *Environmental Research Letters* 3 (1) (2008) 1–5.
[4] E. Pedersen, L.-M. Hallberg, K.P. Waye, Living in the vicinity of wind turbines—a grounded theory study, *Qualitative Research in Psychology* 4 (1–2) (2007) 49–63.
[5] G. Van den Berg, The beat is getting stronger: *the effect of atmospheric stability on low frequency modulated sound of wind turbines*, *Journal of Low Frequency Noise, Vibration and Active Control* 24 (1) (2005) 1–24.
[6] C. Doolan, D.J. Moreau, L.A. Brooks, Wind turbine noise mechanisms and some concepts for its control, *Acoustics Australia* 40 (1) (2012) 7–13.
[7] N. Curle, The influence of solid boundaries upon aerodynamic sound, *Proceedings of the Royal Society of London Series A: Mathematical and Physical Sciences* 231 (1187) (1955) 505–514.
[8] N.D. Kelley, H. McKenna, R. Hemphill, C. Etter, R. Garrelts, N. Linn, Acoustic Noise Associated With the Mod-1 Wind Turbine: Its Source, Impact, and Control, Technical Report, US Department of Energy, 1985.
[9] M. Goldstein, *Aeroacoustics*, McGraw-Hill, New York, USA, 1976.
[10] RenewableUK, Wind Turbine Amplitude Modulation: Research to Improve Understanding as to its Cause and Effect, Technical Report, 2013.

[11] S. Oerlemans, Effect of wind shear on amplitude modulation of wind turbine noise, *International Journal of Aeroacoustics* 14 (5–6) (2015) 715–728.
[12] G. Van den Berg, Effects of the wind profile at night on wind turbine sound, *Journal of Sound and Vibration* 277 (4) (2004) 955–970.
[13] K. Hansen, B. Zajamšek, C. Hansen, Identification of low frequency wind turbine noise using secondary windscreens of various geometries, *Noise Control Engineering Journal* 62 (2) (2014) 69–82.
[14] J. Jakobsen, Infrasound emission from wind turbines, *Low Frequency Noise, Vibration and Active Control* 24 (3) (2005) 145–155.
[15] C. Turnbull, J. Turner, D. Walsh, Measurement and level of infrasound from wind farms and other sources, *Acoustics Australia* 40 (1) (2012) 45–50.
[16] R.D. O'Neal, R.D. Hellweg, R.M. Lampeter, Low frequency noise and infrasound from wind turbines, *Noise Control Engineering Journal* 59 (2) (2011) 135–157.
[17] S.S. Jung, W.-S. Cheung, C. Cheong, S.-H. Shin, Experimental identification of acoustic emission characteristics of large wind turbines with emphasis on infrasound and low-frequency noise, *Journal of the Korean Physical Society* 53 (4) (2008) 1897–1905.
[18] H. Møller, C.S. Pedersen, Low-frequency noise from large wind turbines, *The Journal of the Acoustical Society of America* 129 (6) (2011) 3727–3744.
[19] O. Marcillo, S. Arrowsmith, P. Blom, K. Jones, On infrasound generated by wind farms and its propagation in low-altitude tropospheric waveguides, *Journal of Geophysical Research: Atmospheres* 120 (19) (2015) 9855–9868.
[20] IEC 61400-11, *Wind Turbine Generator Systems—Part 11: Acoustic Noise Measurement Techniques*, International Electrotechnical Commission, Geneva, Switzerland, 2012.
[21] L. Kjaergaard, Microphone Halt Report, Technical Report, G.R.A.S., 2015.
[22] Australian Energy Market Operator, ⟨http://www.aemo.com.au/Electricity/Market-Operations/Dispatch/AWEFS⟩ (accessed: 17/12/2015).
[23] R. Randall, Application of B&K Equipment to Frequency Analysis, 2nd edition, Technical Report, B&K, 1977.
[24] S. Pedersen, H. Møller, K.P. Waye, Indoor measurements of noise at low frequencies-problems and solutions, *Journal of Low Frequency Noise, Vibration & Active Control* 26 (4) (2007) 249–270.
[25] G. Van den Berg, Wind turbine power and sound in relation to atmospheric stability, *Wind Energy* 11 (2) (2008) 151–169.
[26] K. Fowler, E. Koppen, K. Matthis, International legislation and regulations for wind turbine noise, *Proceedings of the Fifth International Meeting on Wind Turbine Noise*, Denver, 2013.
[27] H.H. Hubbard, Aeroacoustics of Flight Vehicles: Theory and Practice, Volume 1. Noise Sources, Technical Report, DTIC Document, 1991.
[28] K.L. Hansen, C.H. Hansen, B. Zajamšek, Outdoor to indoor reduction of wind farm noise for rural residences, *Building and Environment* 94 (2) (2015) 764–772.
[29] N. Sawalhi, R.B. Randall, Gear parameter identification in a wind turbine gearbox using vibration signals, *Mechanical Systems and Signal Processing* 42 (1) (2014) 368–376.
[30] ISO 226, *Normal Equal-Loudness Level Contours*, International Organization for Standardization, Genéve, 2003.
[31] South Australian Environmental Protection Authority (SA EPA), *Waterloo Wind Farm Environmental Noise Study*, 2013.
[32] S. Lee, K. Kim, W. Choi, S. Lee, Annoyance caused by amplitude modulation of wind turbine noise, *Noise Control Engineering Journal* 59 (1) (2011) 38–46.
[33] K.I. Hume, M. Brink, M. Basner, et al., Effects of environmental noise on sleep, *Noise and Health* 14 (61) (2012) 297.
[34] A.N. Salt, T.E. Hullar, Responses of the ear to low frequency sounds, infrasound and wind turbines, *Hearing Research* 268 (1) (2010) 12–21.
[35] R.B. Stull, *An Introduction to Boundary Layer Meteorology*, Kluwer Academic Publishers, Dordrecht, The Netherlands, 1988.
[36] H.H. Hubbard, K.P. Shepherd, Aeroacoustics of large wind turbines, *The Journal of the Acoustical Society of America* 89 (6) (1991) 2495–2508.
[37] G.L. Leishman, *Principles of Helicopter Aerodynamics*, Cambridge University Press, New York, USA, 2006.